Electronic Supplementary Material (ESI) for Dalton Transactions.

Anion complexation with cyanobenzoyl substituted first and second generation tripodal amide receptors: crystal structures and solution studies

Md. Najbul Hoque, Abhijit Gogoi and Gopal Das*

Department of Chemistry, Indian Institute of Technology Guwahati, Assam-781039,

Fax: +91-361-2582349; Tel: +91-361-2582313; E-mail: gdas@iitg.ernet.in.

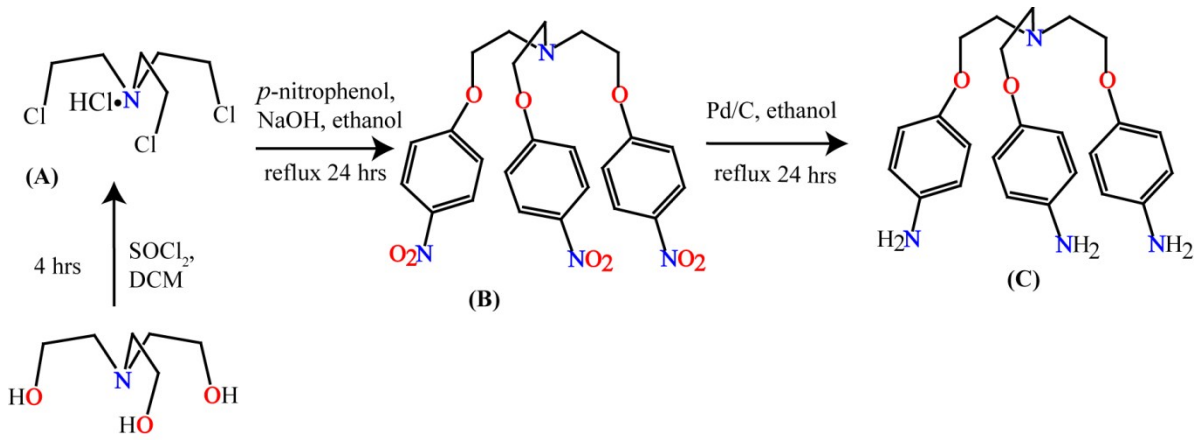

Scheme S1. Preparation of tripodal amine C.

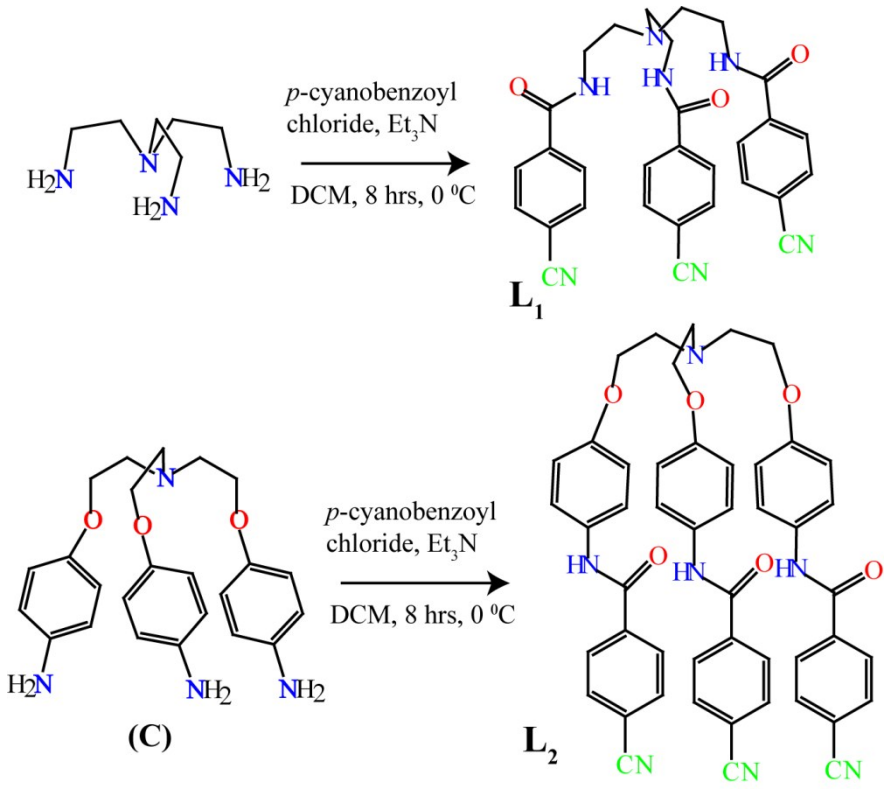

Scheme S2. Preparation of tripodal amide receptors $\mathbf{L_1}$ and $\mathbf{L_2}$.

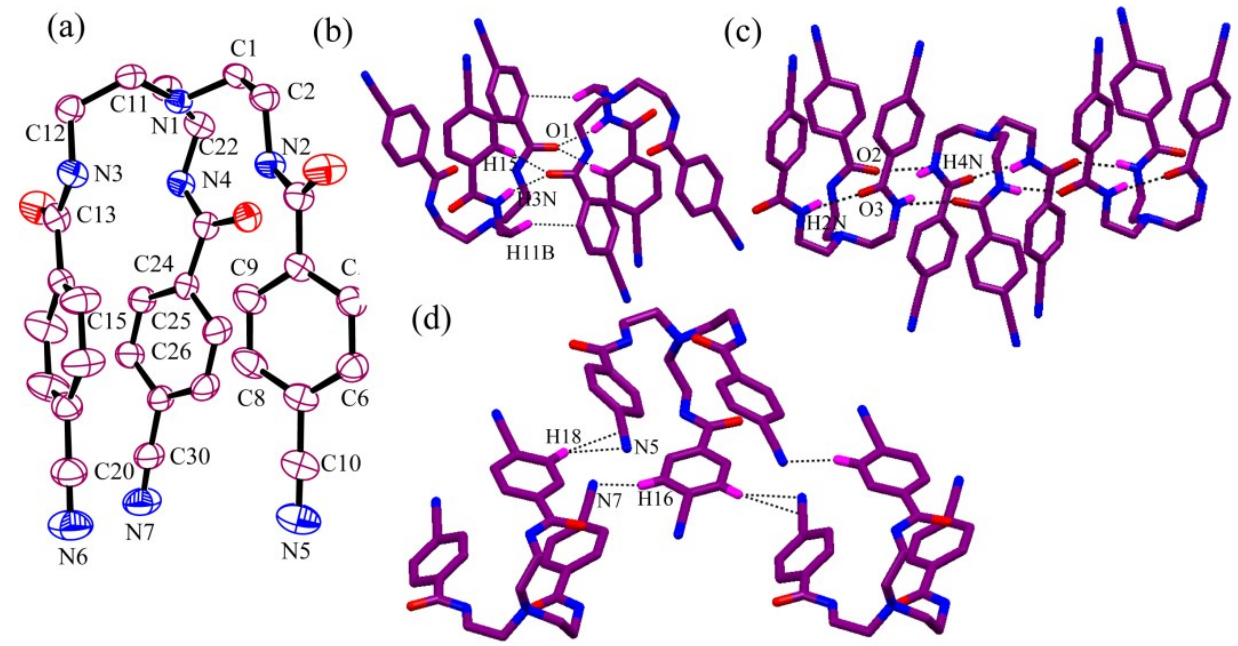

Fig. S1 (a) ORTEP drawing of free receptor $\mathbf{L_1}$ with thermal ellipsoid at the 30% probability. (b) A N···H−O and C···H−O H-bonded dimeric unit of $\mathbf{L_1}$. (c) Intra and intermolecular N···H−O H-bonded 1-D assembly. (d) C−H···N and C−H···π interaction of electron rich -CN group.

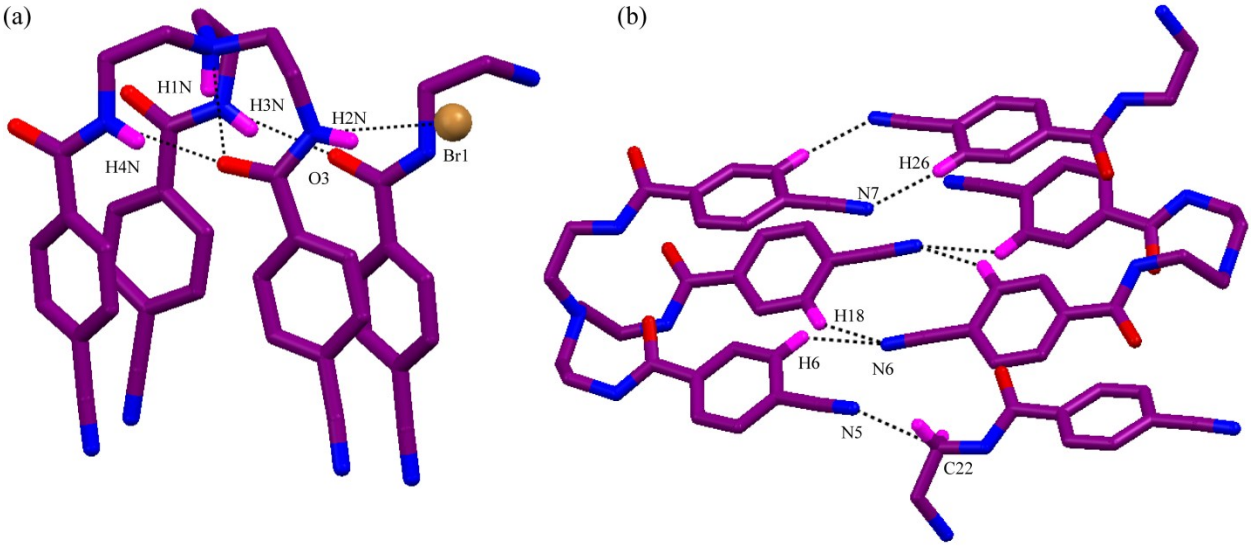

Fig. S2 (a) Mercury structure depicting the conformation of the protonated receptor and intra and intermolecular H-bonding of amide hydrogen in complex **2**. (b) Snapshot showing intermolecular H-bonding among –CN group and CH hydrogen connecting layers.

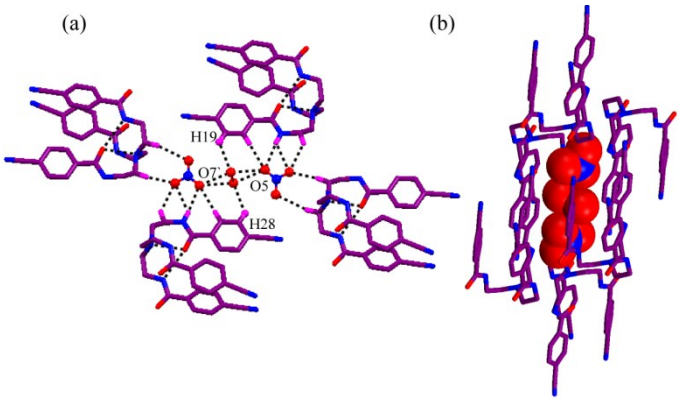

Fig. S3 (a) A close view of $[(NO_3^-)_2\text{-}(H_2O)]^{4-}$ cluster and H-bonding interaction of water molecule in complex **4**. (b) A nitrate-water cluster $[(NO_3^-)_2\text{-}(H_2O)]^{4-}$ encapsulated in cationic cavity created by six $\mathbf{L_1H^+}$ receptors.

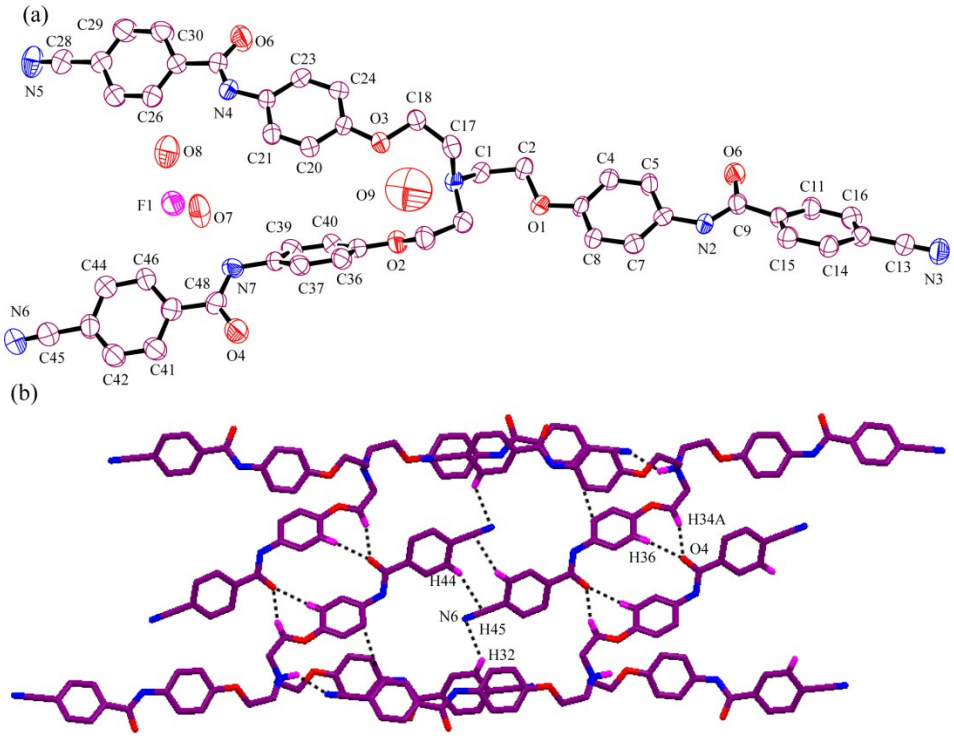

Fig. S4 (a) ORTEP drawing of fluoride complex **6** of $\mathbf{L_2}$ with thermal ellipsoid at the 30% probability. (b) 1D aggregation of the pseudocapsular complex and interaction between two layers.

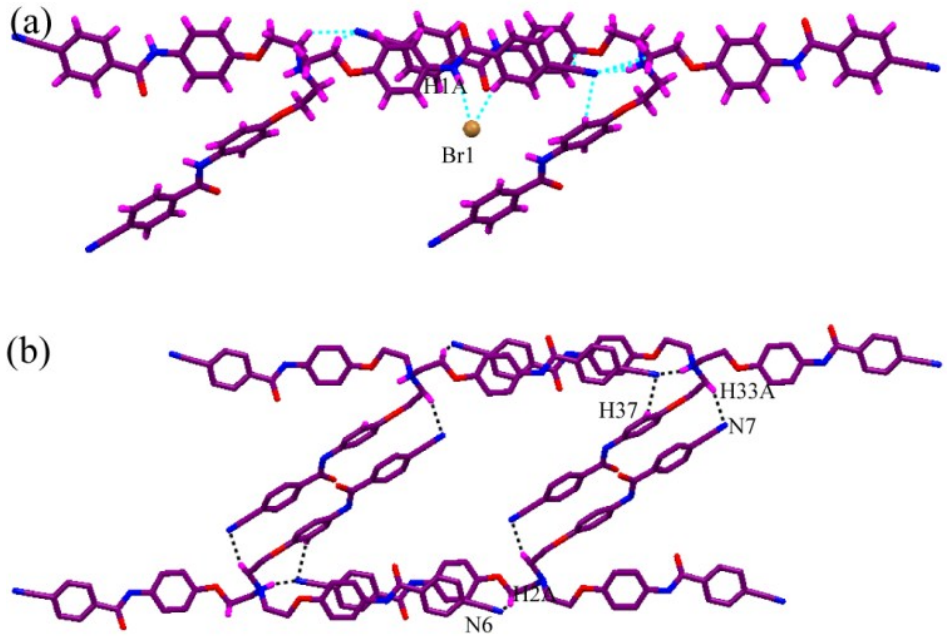

Fig. S5 (a) Pseudocapsular assembly and interaction of bromide ion in complex **7**. (b) 1D assembly of C−H···N connected pseudocapsular layer.

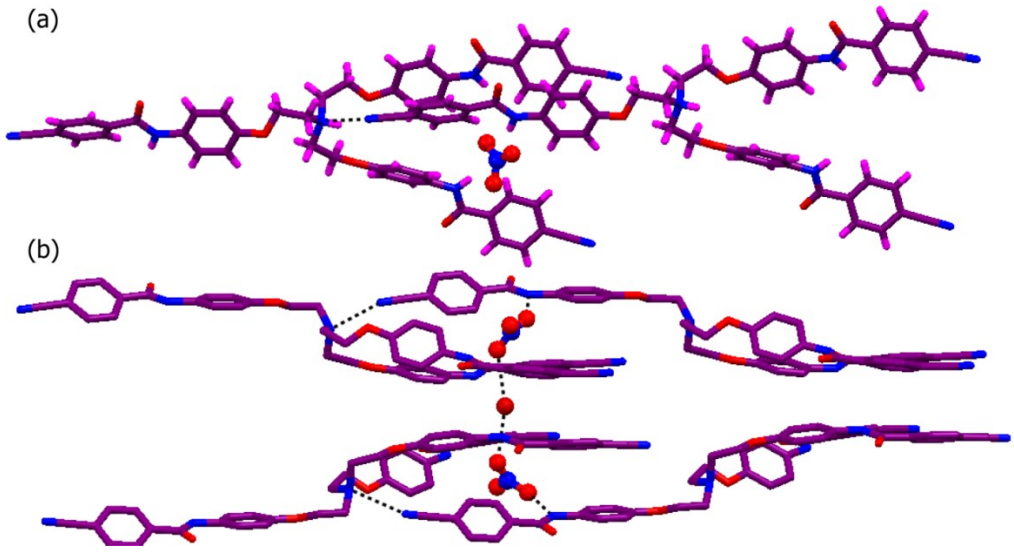

Fig. S6 (a) Crystal structure of complex **8** depicting the formation of pseudocapsular cavity containing NO_3^- ion. (b) Nitrate-water cluster $[(NO_3)_2\text{-}H_2O)]^{2-}$ passing through two pseudocapsular cavity.

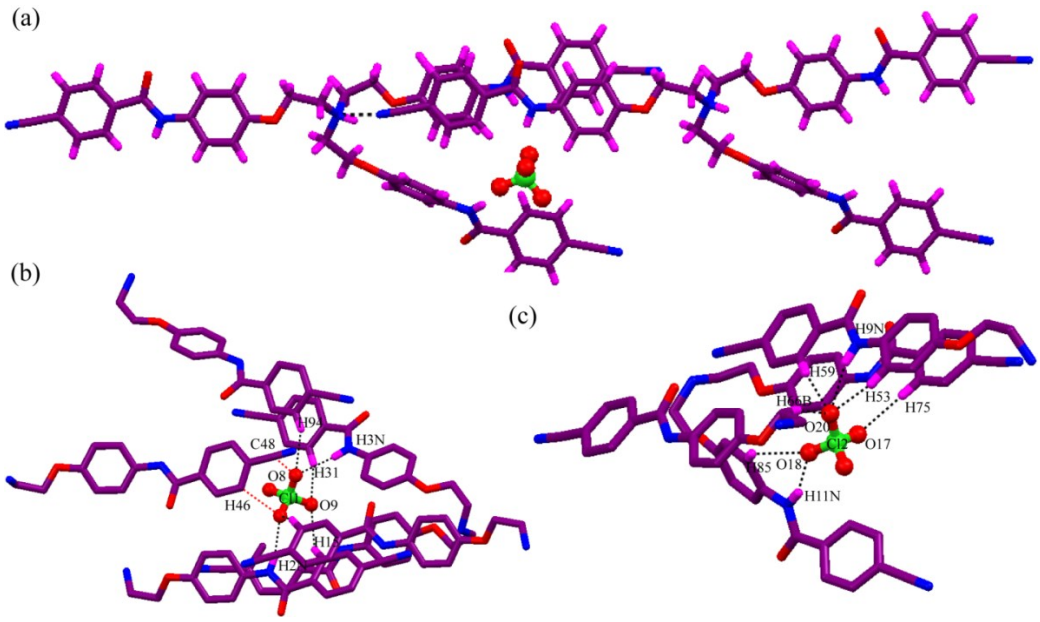

Fig. S7 (a) Crystal structure of complex **9** depicting the formation of pseudocapsular cavity containing ClO_4^- ion. (b) and (c) Partial view of the eight and seven co-ordinations of two symmetry independent $Cl(1)O_4^-$ and $Cl(2)O_4^-$ ion respectively.

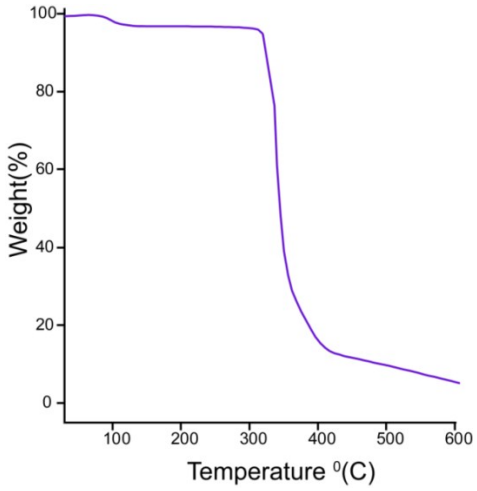

Fig. S8 Thermogravimetric analysis (TGA) curve of **$[(L_1H)_2{\cdot}2NO_3{\cdot}H_2O]$(4)** at a heating rate of 5 °C per min. the nitrate complex **4** of first generation tripodal **L_1** contains water molecule and shows charatctics weight loss at 100 ºC.

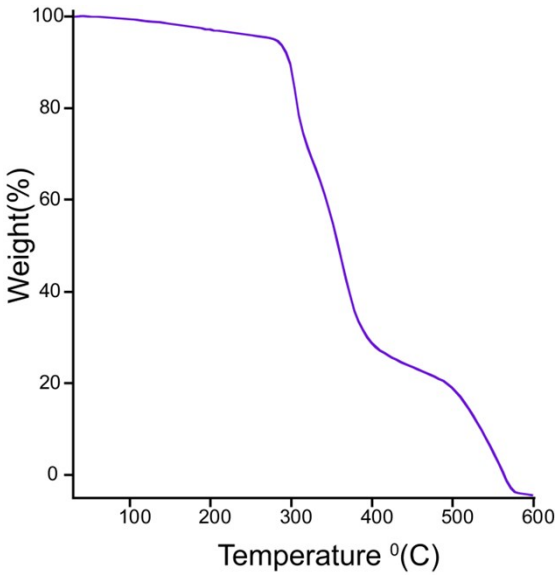

Fig. S9 Thermogravimetric analysis (TGA) curve of **[L_1H·ClO_4](5)** at a heating rate of 5 °C per min. TGA experiment of the free receptor **L_1** and the other complexes did not give any significant results. So here we only produced the TGA spectra of perchlorate complex and nitrate complex as a reference.

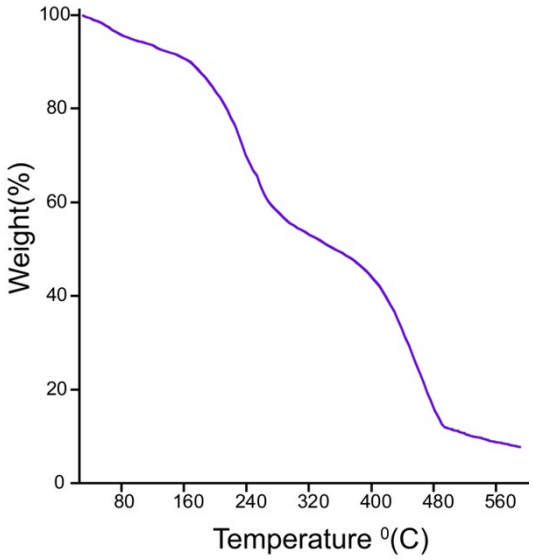

Fig. S10 In case of bromide complex we could not assign the solvent molecules, hence PLATON/SQUEEZE was performed to refine the receptor along with the bromide ion (1.5 Br

ion) by excluding the disordered solvent electron densities. This calculated amount of 554 electrons per unit cell or 98 electrons per molecule may be attributed to two water and two DMF molecules. Thermogravimetric analysis (TGA) curve of **[L_2H·Br](7)** at a heating rate of 5 °C per min. Platon/Squeeze was carried out to exclude undefined electrons and to justify the crystallographic findings the TGA experiment was done. Thermal Analysis performed on dried crystals of bromide complex **7**; indicate the loss of two water and two DMF molecules with a weight 15.36 % (Calcd. 16.23 %) as multi-step process from 85 ºC and 185 ºC.

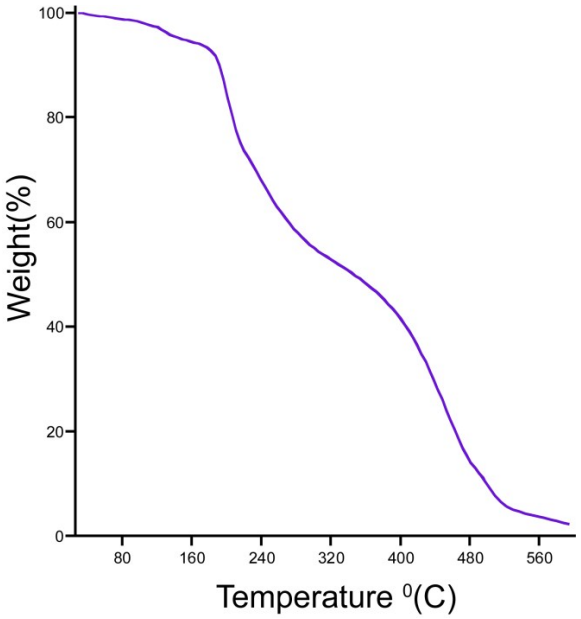

Fig. S11 In this case there exists certain amount of DMF-water solvent trapped in the crystal lattice in a disordered manner. These electron densities were moved during refinement and the count of electron removed in total was 226 per two symmetry independent molecules which account for five DMF and three water molecules. Thermogravimetric analysis (TGA) curve of **[L_2H·ClO_4](9)** at a heating rate of 5 °C per min. Platon/Squeeze was carried out to exclude undefined electrons and to justify the crystallographic findings the TGA experiment was done. Thermal Analysis performed on dried crystals of perchlorate complex **9**; indicate the loss

of three water and five DMF molecules with a weight 3.01 % (Calcd. 2.5 %) as multi-step process from 80 ºC and 170 ºC.

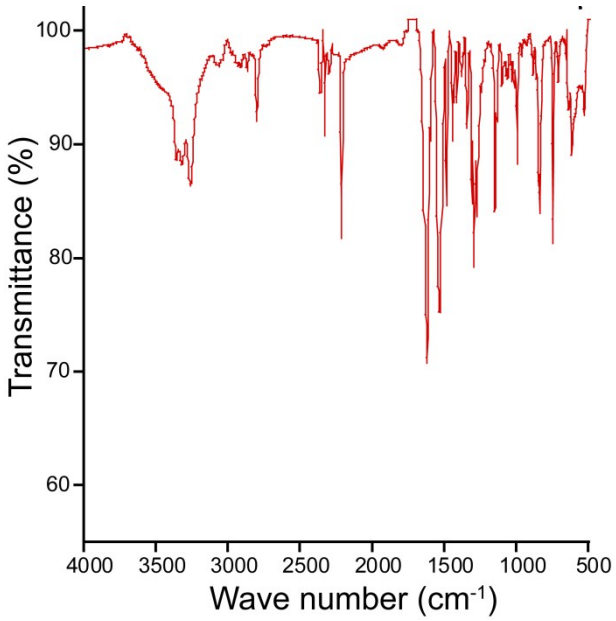

Fig. S12 FTIR spectrum of **L_1(1)**.

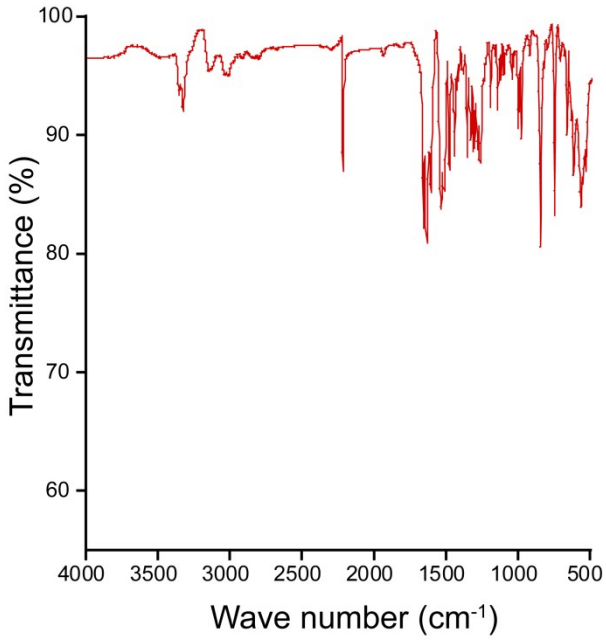

Fig. S13 FTIR spectrum of **[L_1H·Br](2)**.

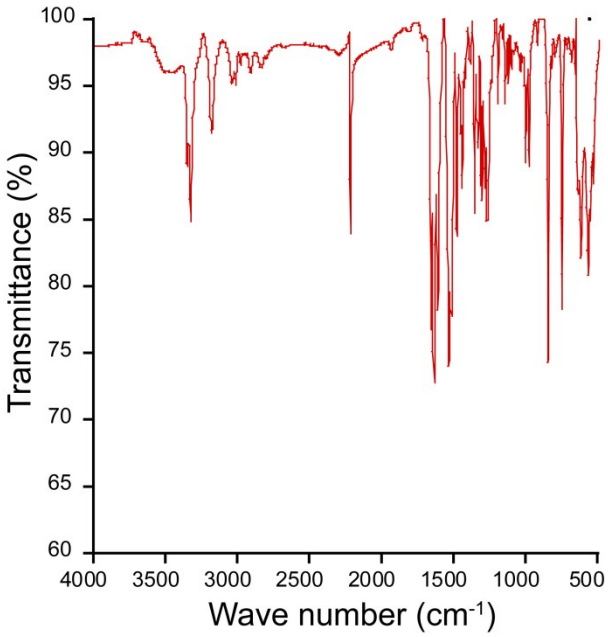

Fig. S14 FTIR spectrum of **[L_1H·I](3)**.

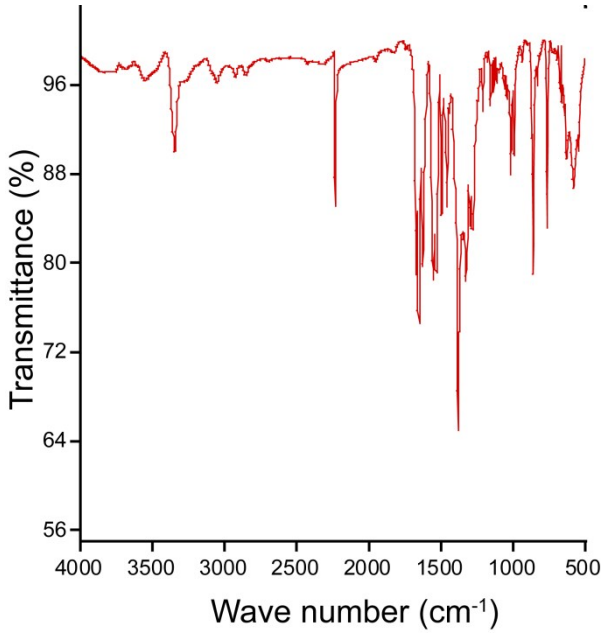

Fig. S15 FTIR spectrum of **[(L_1H)$_2$·2NO_3·H_2O](4)**.

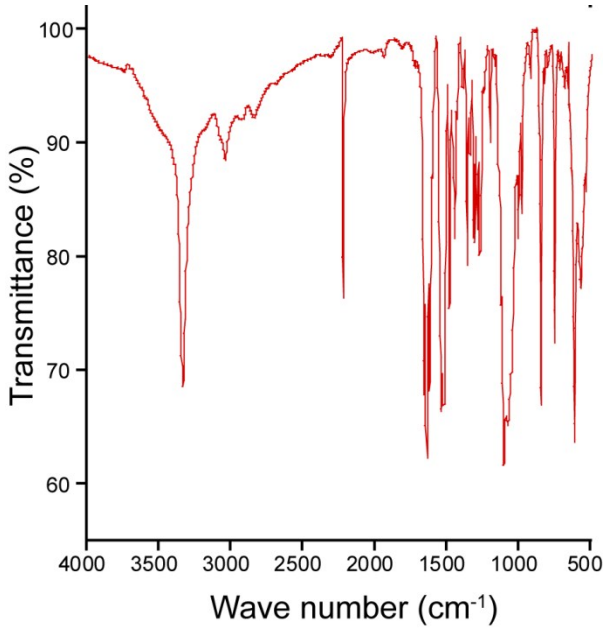

Fig. S16 FTIR spectrum of **[L_1H·ClO_4](5)**.

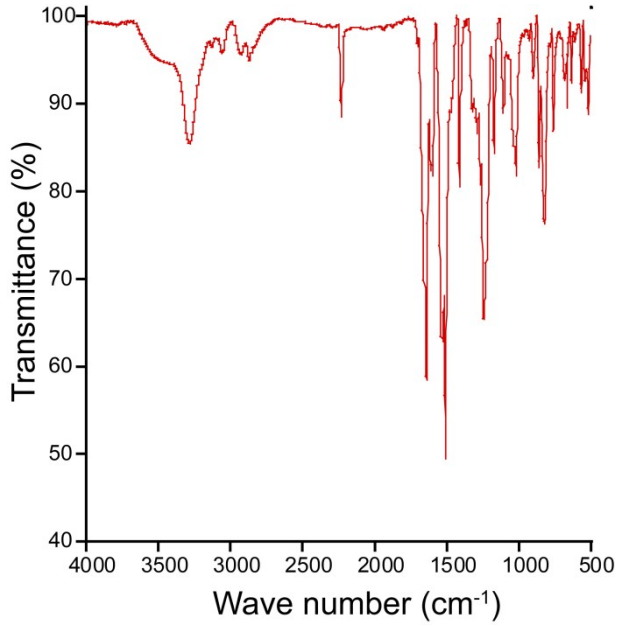

Fig. S17 FTIR spectrum of $\mathbf{L_2}$.

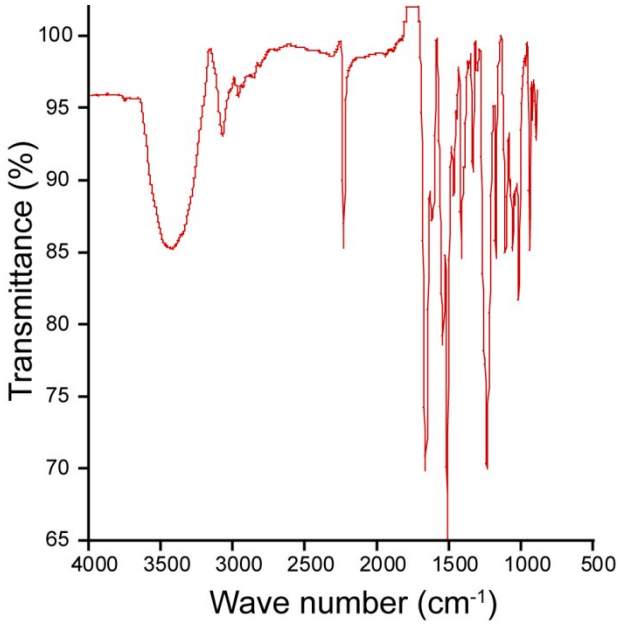

Fig. S18 FTIR spectrum of **[4LH·4HF$_2$·3H$_2$O](6)**

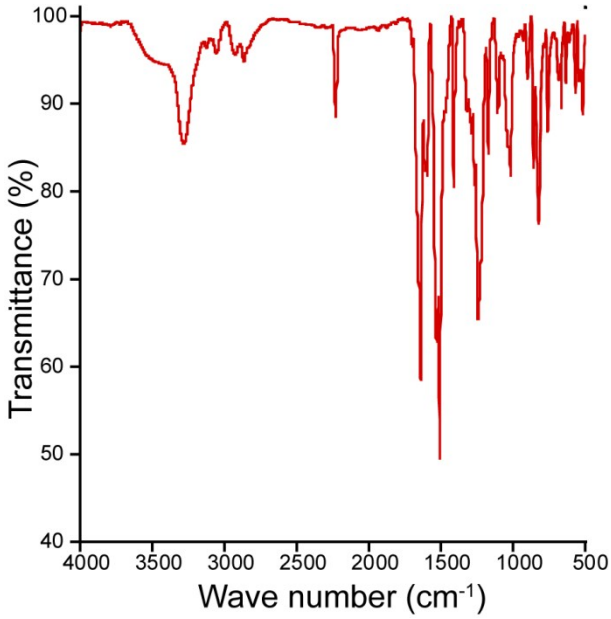

Fig. S19 FTIR spectrum of **[L$_2$H·Br](7)**.

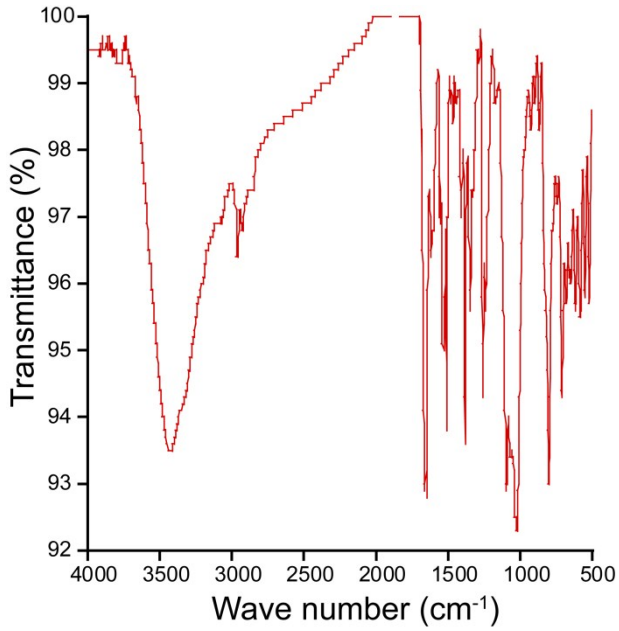

Fig. S20 FTIR spectrum of **[$L_2H{\cdot}NO_3{\cdot}H_2O$](8)**.

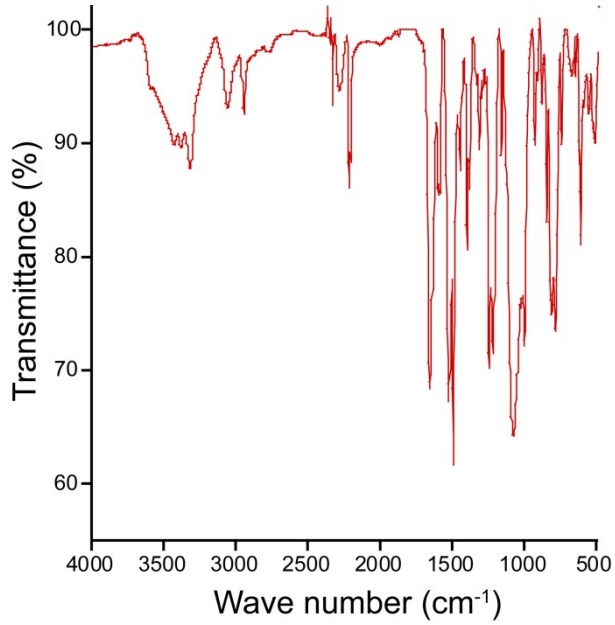

Fig. S21 FTIR spectrum of **[$L_2H{\cdot}ClO_4$](9)**.

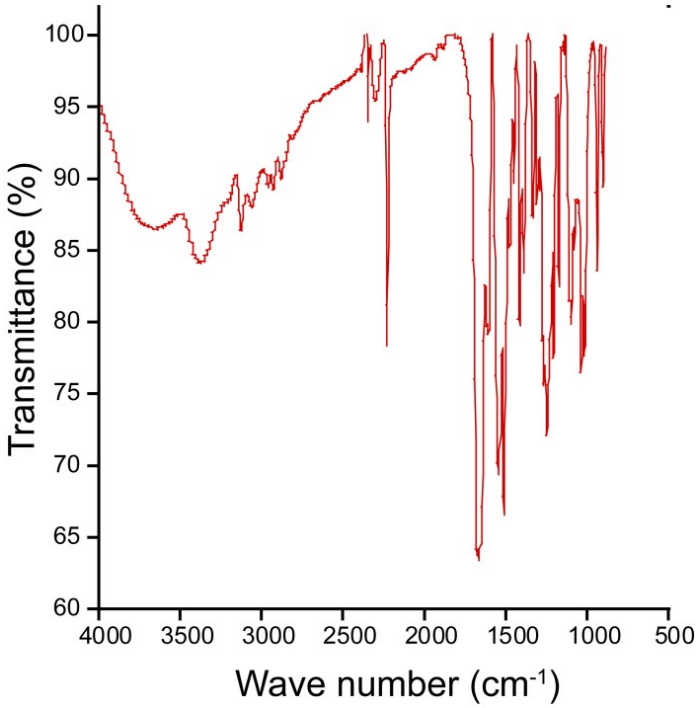

Fig. S22 FTIR spectrum of **[$(L_2H)_2$·SIF_6·$4H_20$·2DMF](10)**.

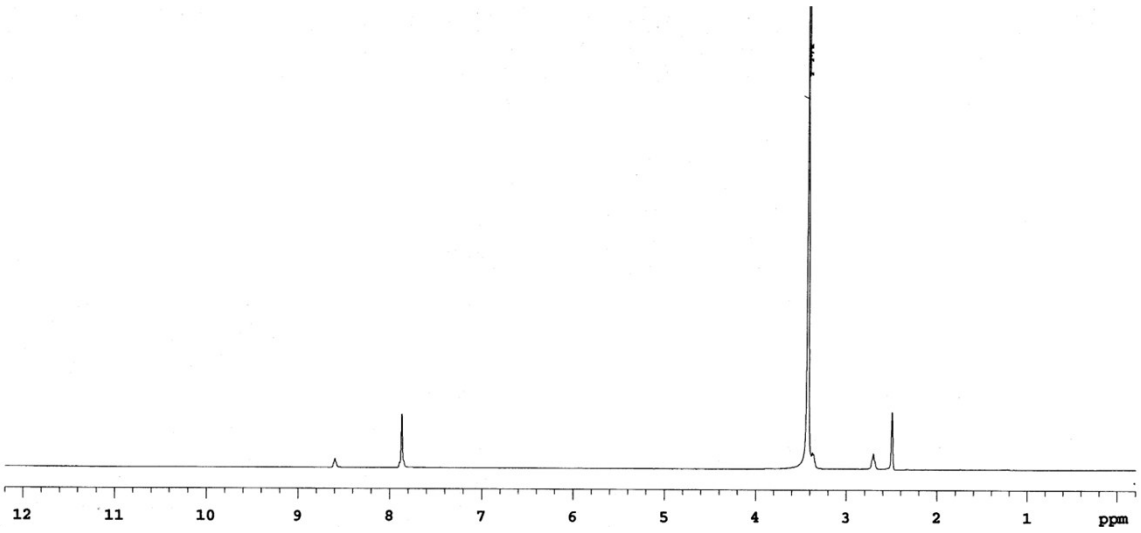

Fig. S23 ^{1}H NMR spectrum of receptor $\mathbf{L_1}$ in DMSO-d_6 at 298 K.

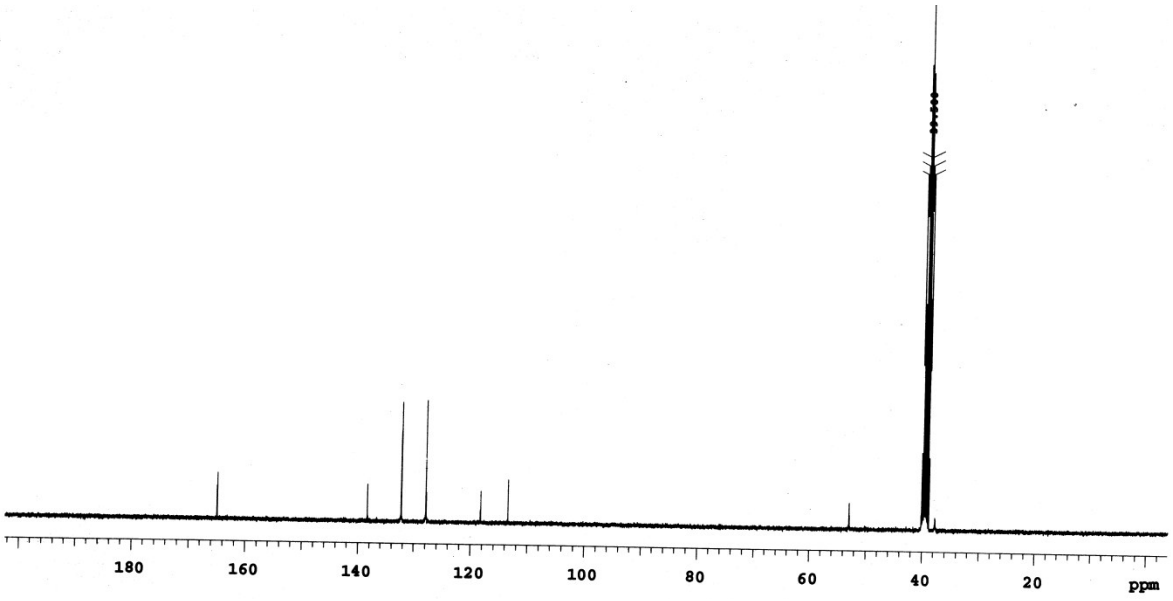

Fig. S24 ^{13}C NMR spectrum of receptor $\mathbf{L_1}$ in DMSO-d_6 at 298 K.

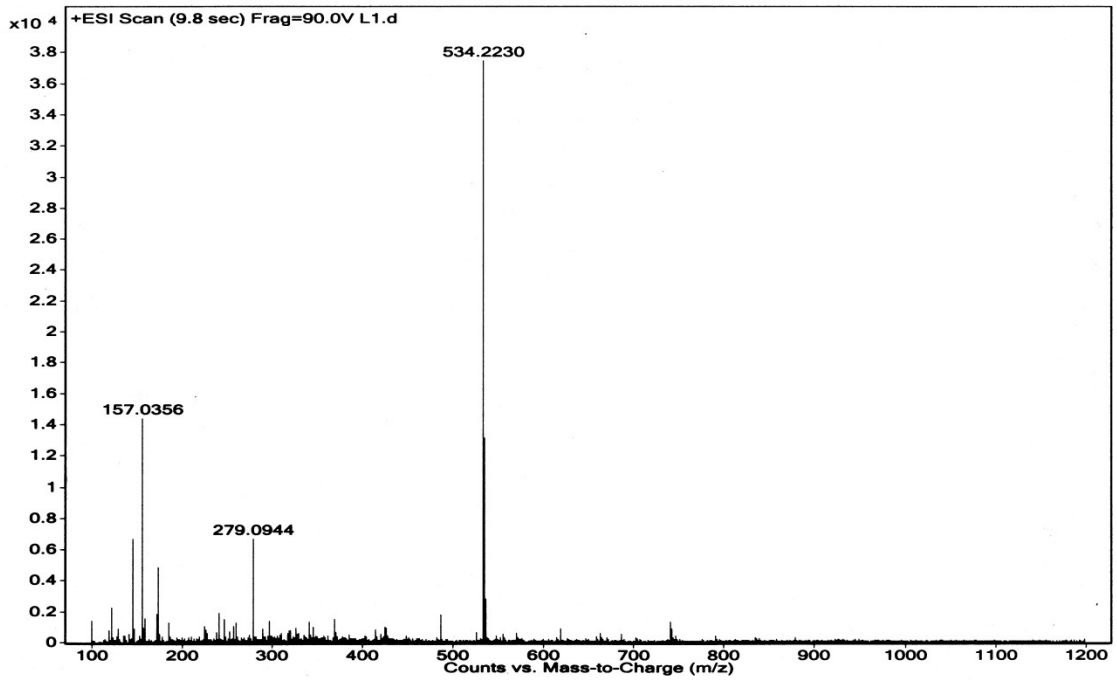

Fig. S25 ESI mass spectra of $\mathbf{L_1}$.

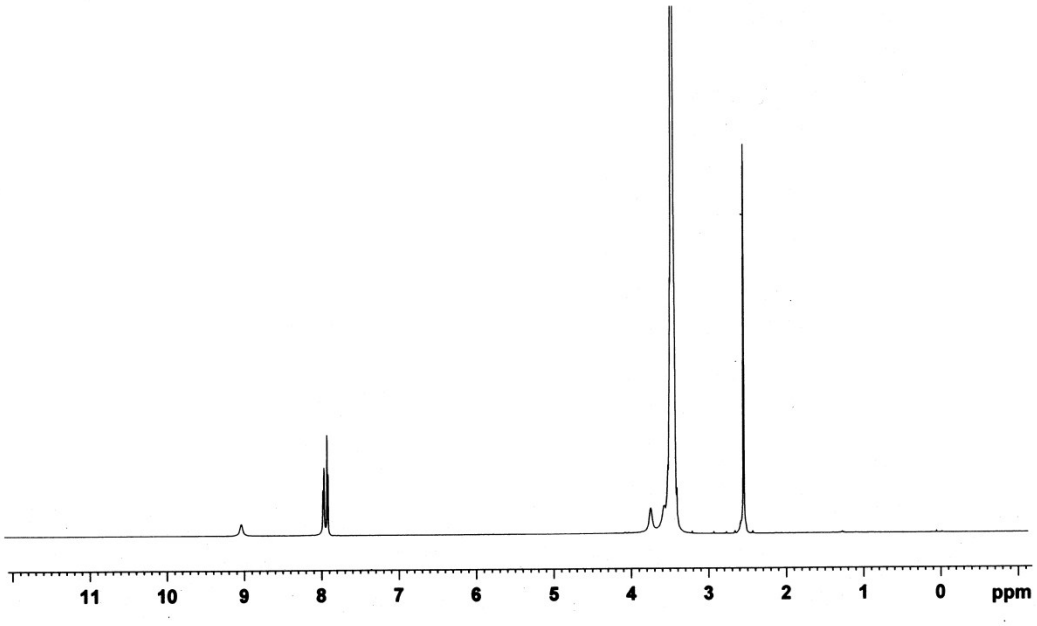

Fig. S26 ^{1}H NMR spectrum of receptor **[L_1H·Br](2)** in DMSO-d_6 at 298 K.

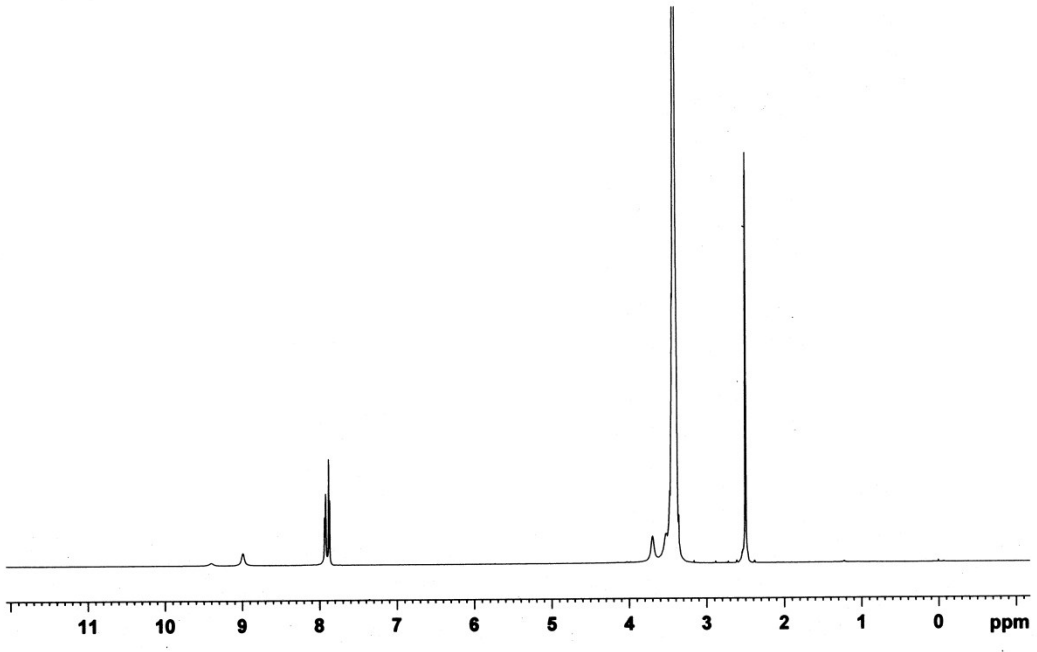

Fig. S27 ^{1}H NMR spectrum of receptor **[L_1H·I](3)** in DMSO-d_6 at 298 K.

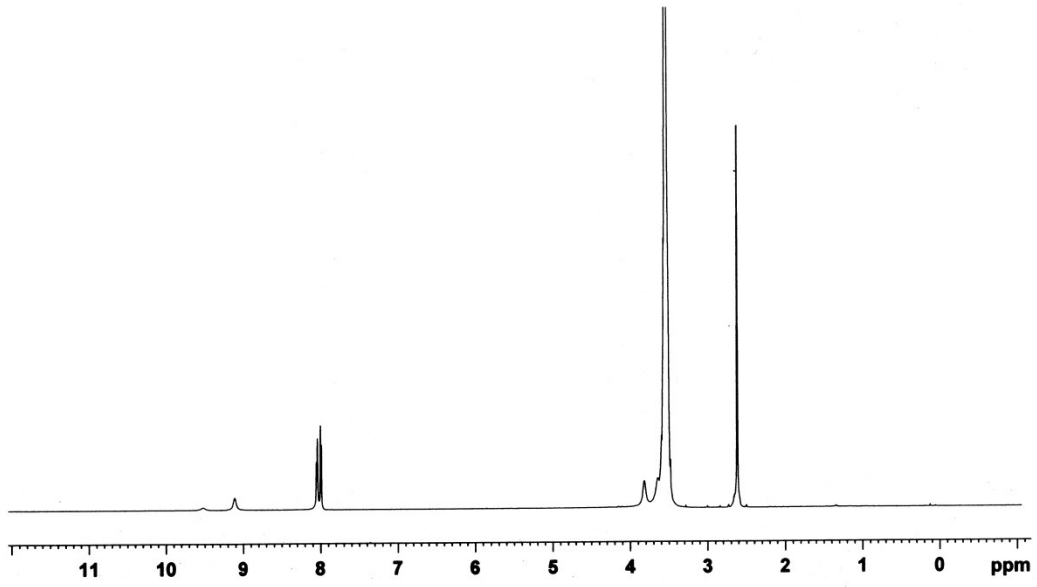

Fig. S28 ^{1}H NMR spectrum of receptor **[$(L_1H)_2 \cdot 2NO_3 \cdot H_2O$](4)** in DMSO-$d_6$ at 298 K.

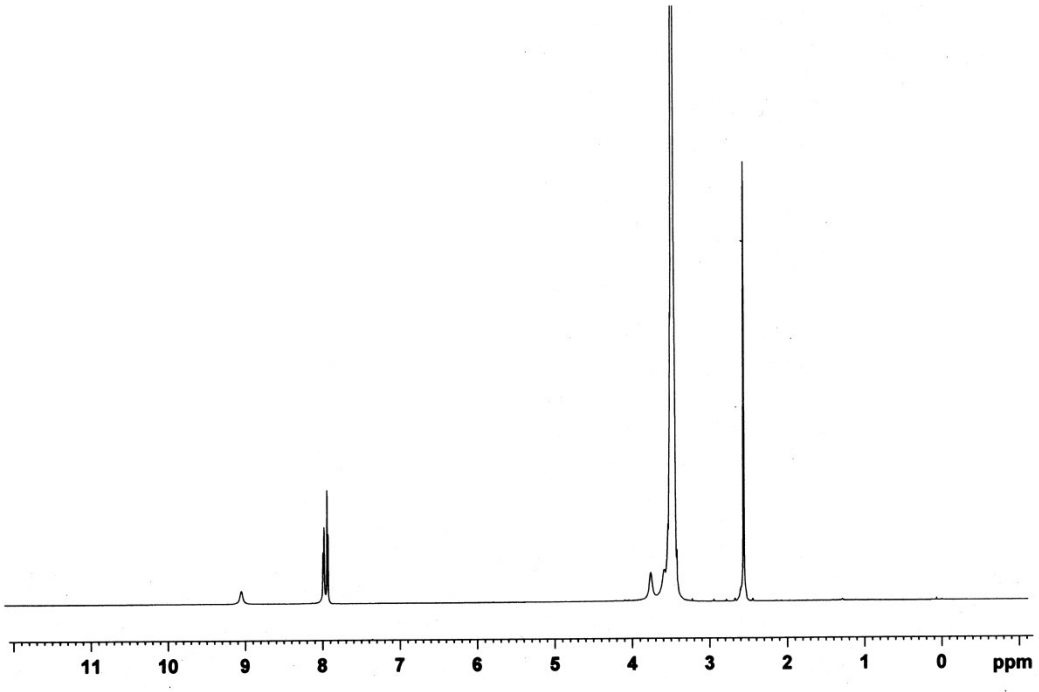

Fig. S29 ^{1}H NMR spectrum of receptor **[$L_1H \cdot ClO_4$](5)** in DMSO-d_6 at 298 K.

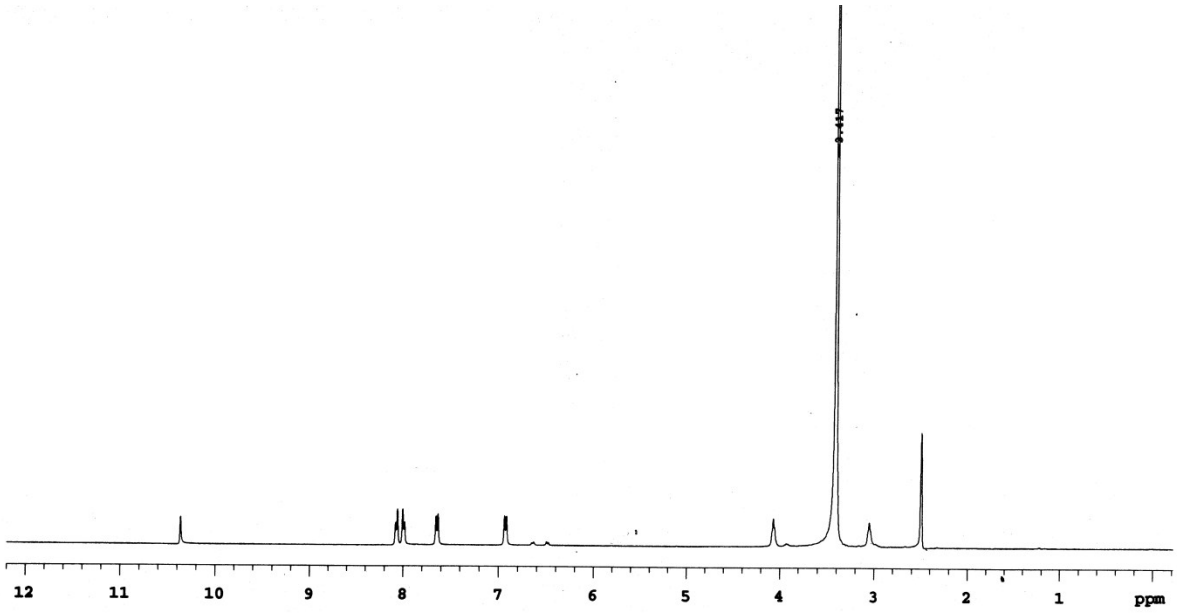

Fig. S30 ^{1}H NMR spectrum of receptor $\mathbf{L_2}$ in DMSO-d_6 at 298 K.

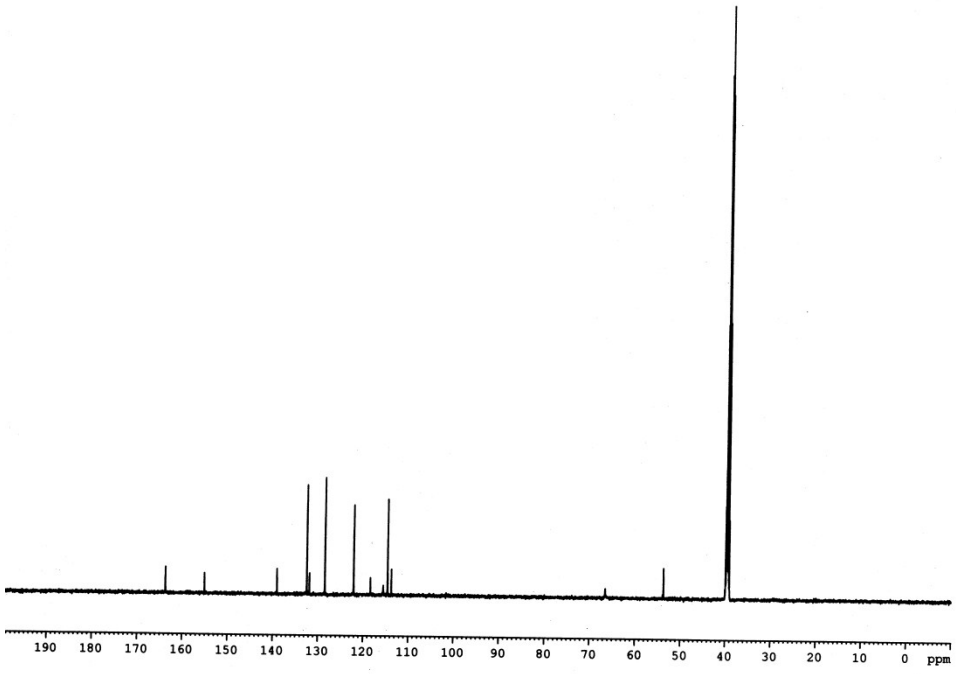

Fig. S31 ^{13}C NMR spectrum of receptor $\mathbf{L_2}$ in DMSO-d_6 at 298 K.

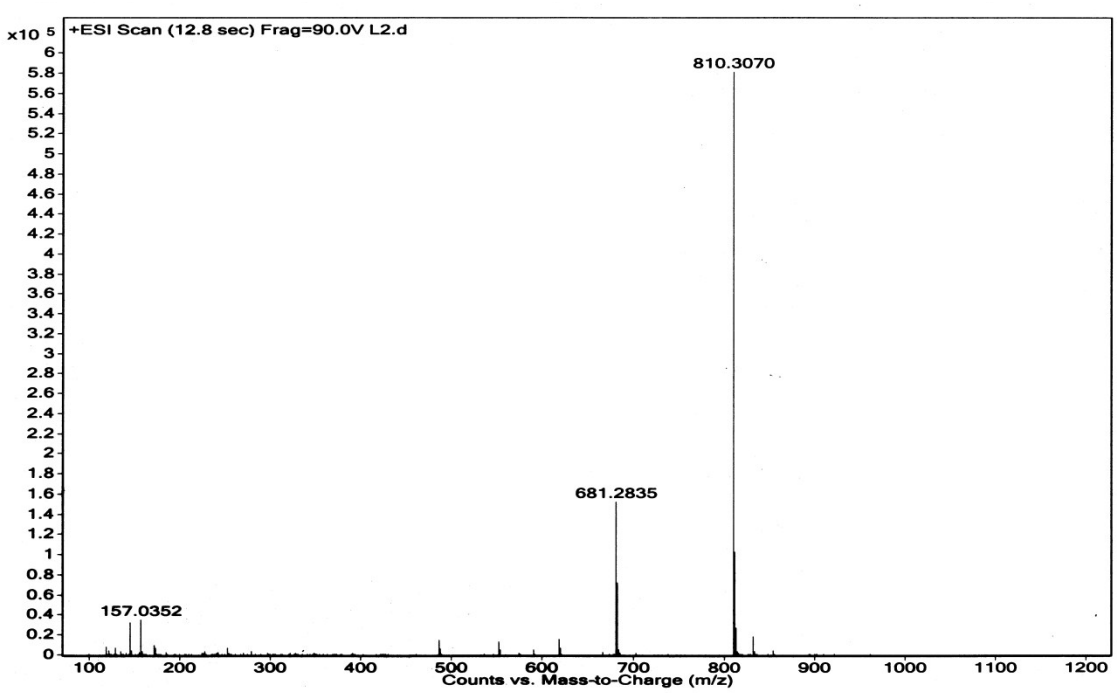

Fig. S32 ESI mass spectra of receptor $\mathbf{L_2}$.

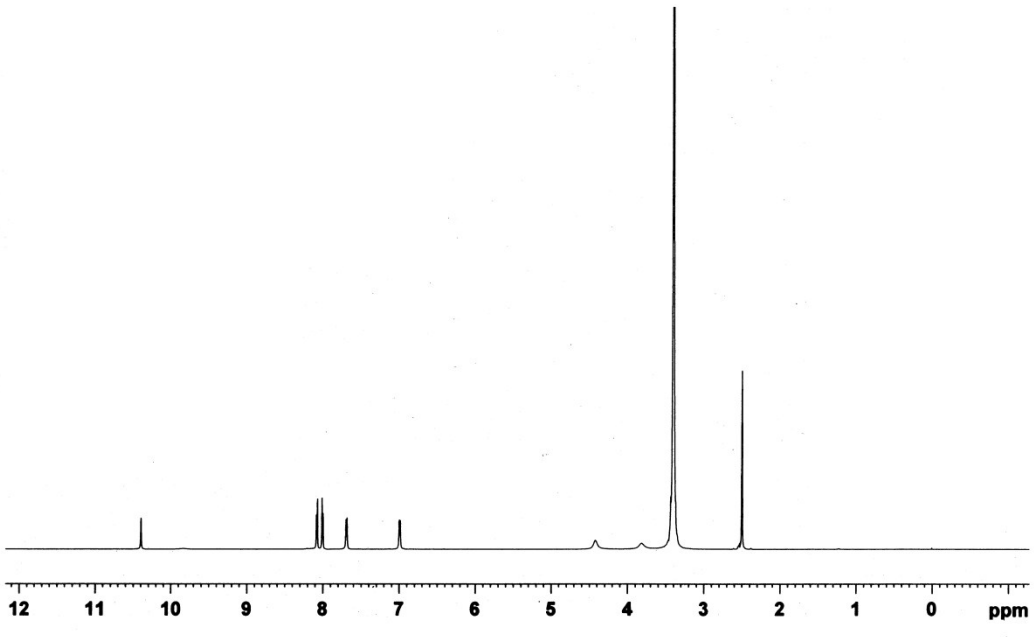

Fig. S33 ^{1}H NMR spectrum of receptor **[4LH·4HF$_2$·3H$_2$O](6)** in DMSO-d_6 at 298 K.

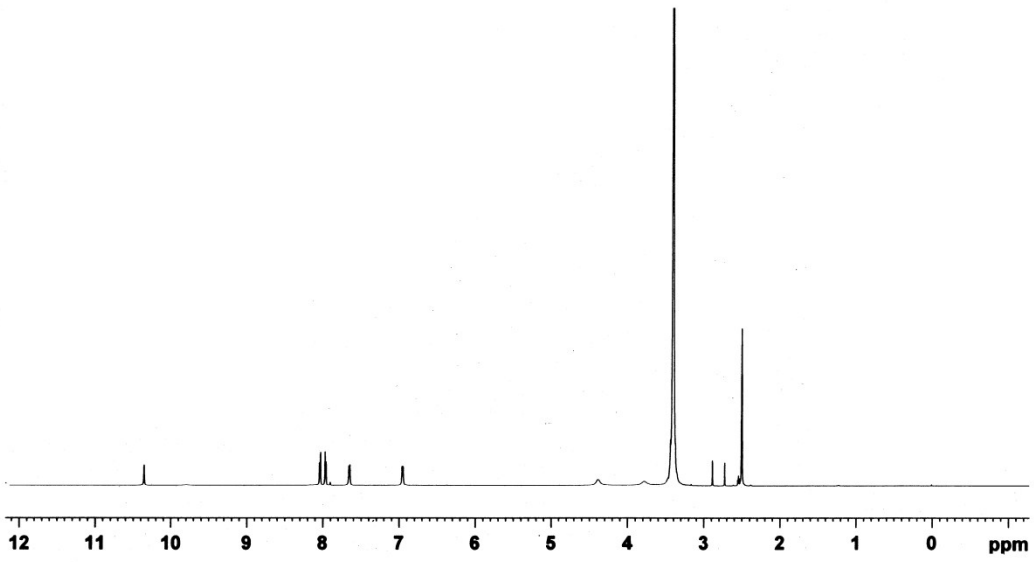

Fig. S34 ^{1}H NMR spectrum of receptor **[L_2H·Br](7)** in DMSO-d_6 at 298 K.

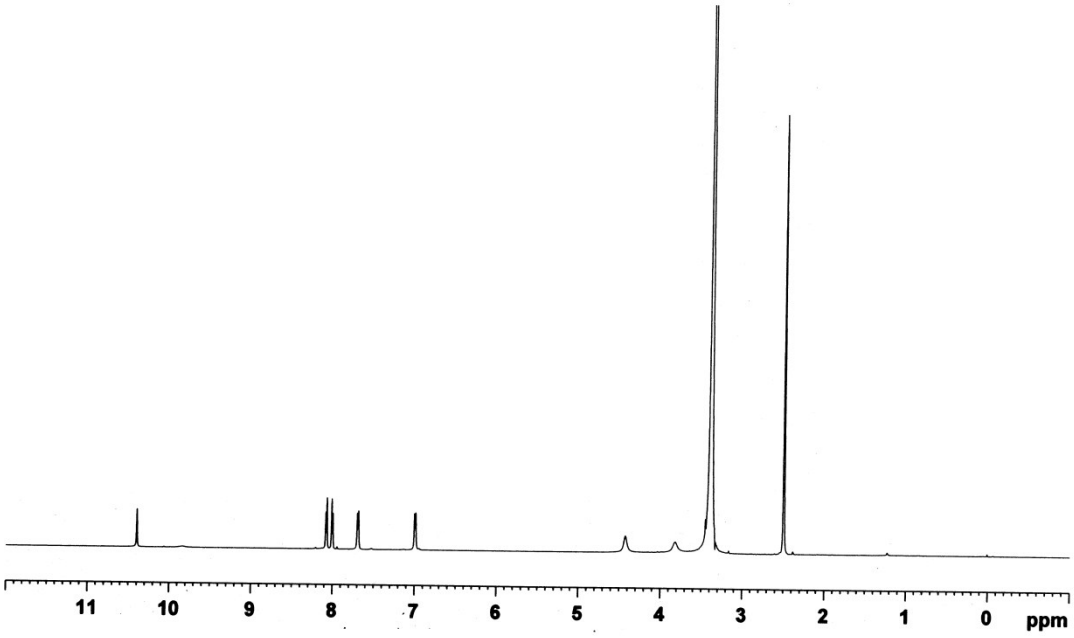

Fig. S35 ^{1}H NMR spectrum of receptor **[l1NO_3·H_2O](8)** in DMSO-d_6 at 298 K.

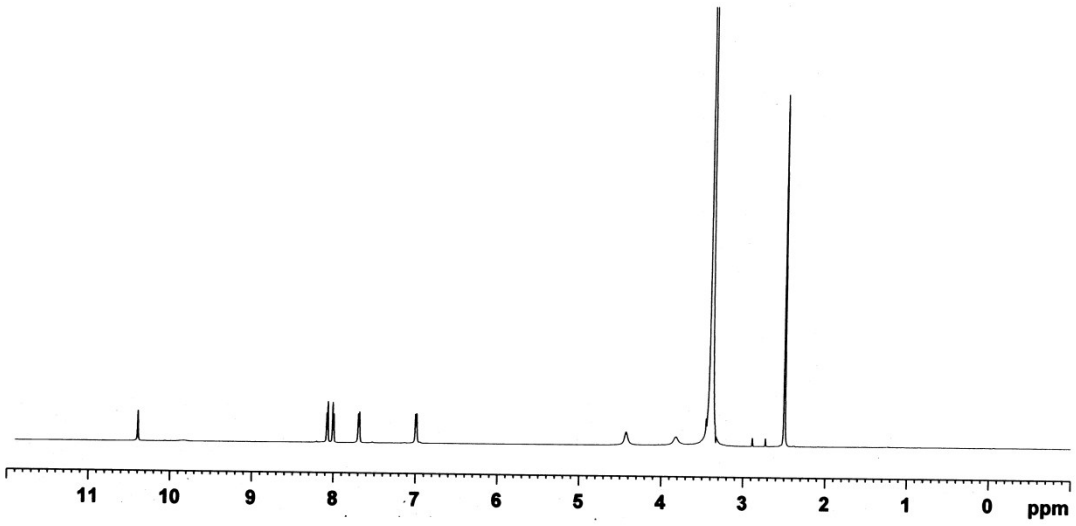

Fig. S36 ^{1}H NMR spectrum of receptor **[$L_2H{\cdot}ClO_4$](9)** in DMSO-d_6 at 298 K.

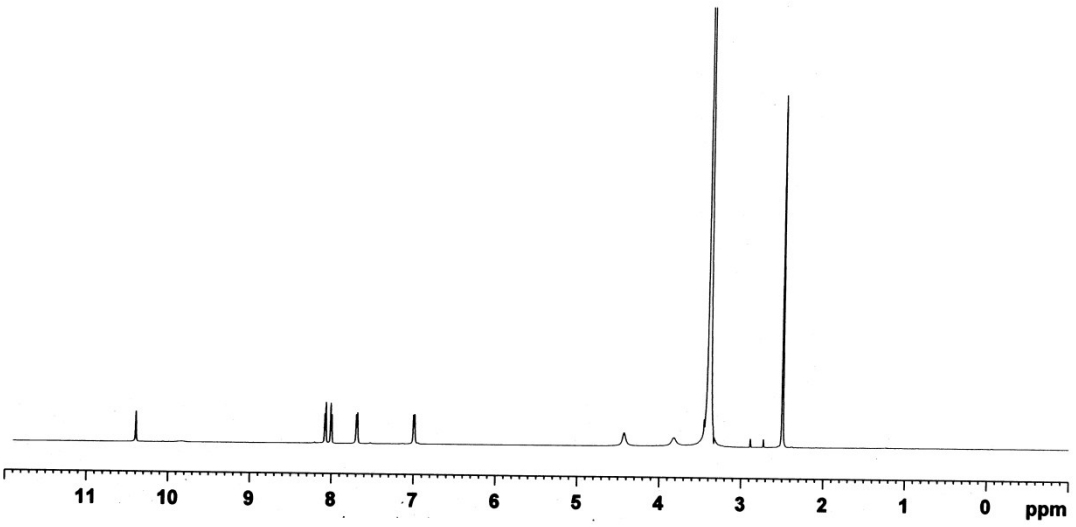

Fig. S37 ^{1}H NMR spectrum of receptor **[$(L_2H)_2{\cdot}SIF_6{\cdot}4H_20{\cdot}2DMF$](10)** in DMSO-$d_6$ at 298 K.

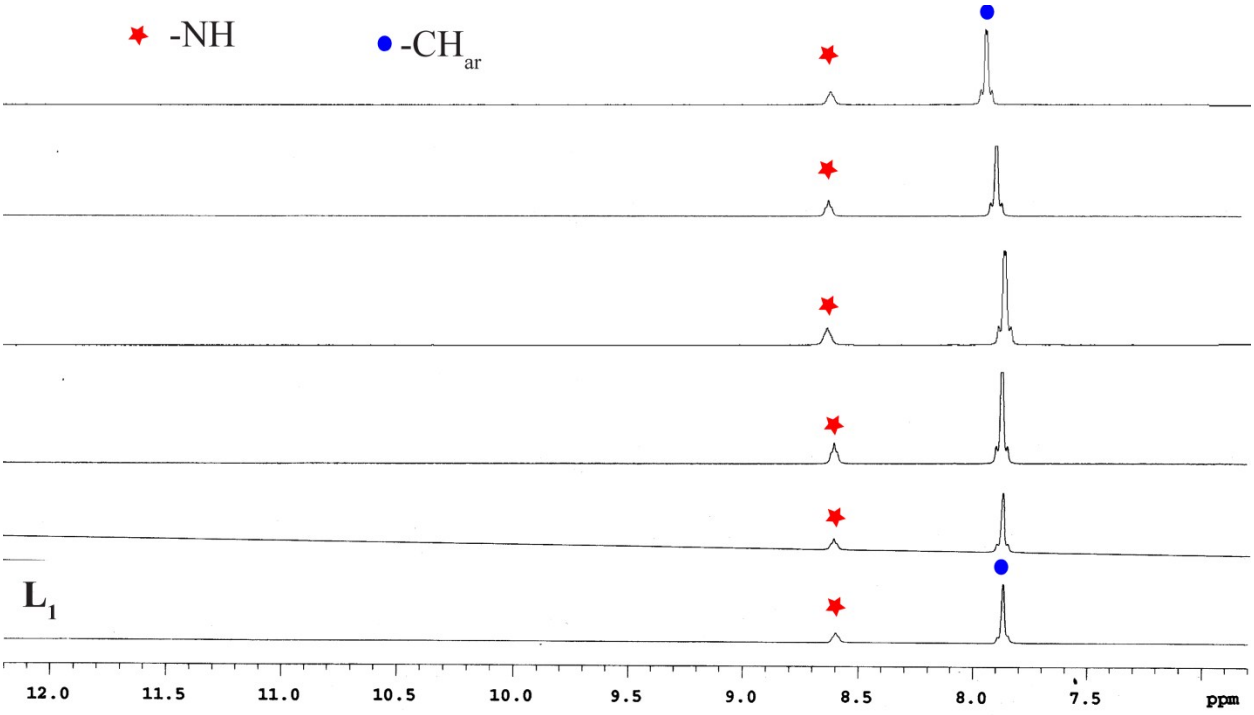

Fig. S38 Stack plot of the ^{1}H NMR spectra of receptor $\mathbf{L_1}$ in the presence of increasing amounts of [*n*-Bu_4N^+]Cl^- recorded in DMSO-d_6 at 298 K.

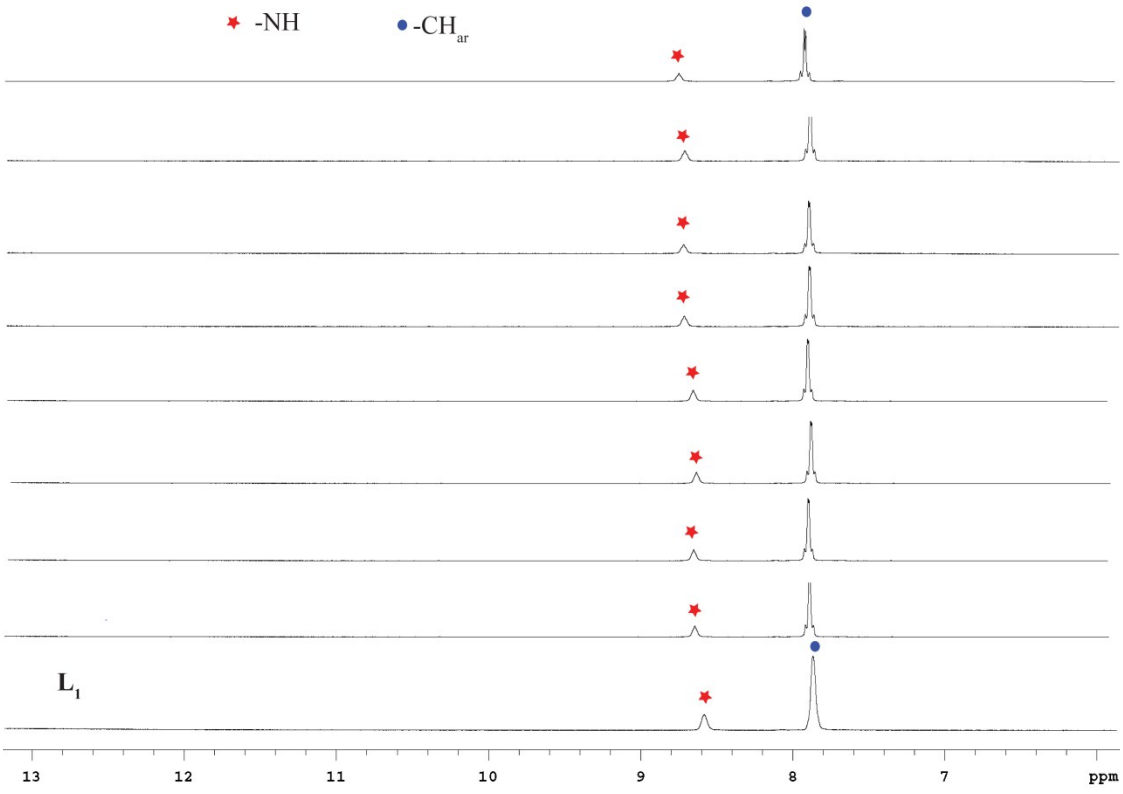

Fig. S39 Stack plot of the ^{1}H NMR spectra of receptor $\mathbf{L_1}$ in the presence of increasing amounts of [*n*-Bu_4N^+]NO_3^- recorded in DMSO-d_6 at 298 K.

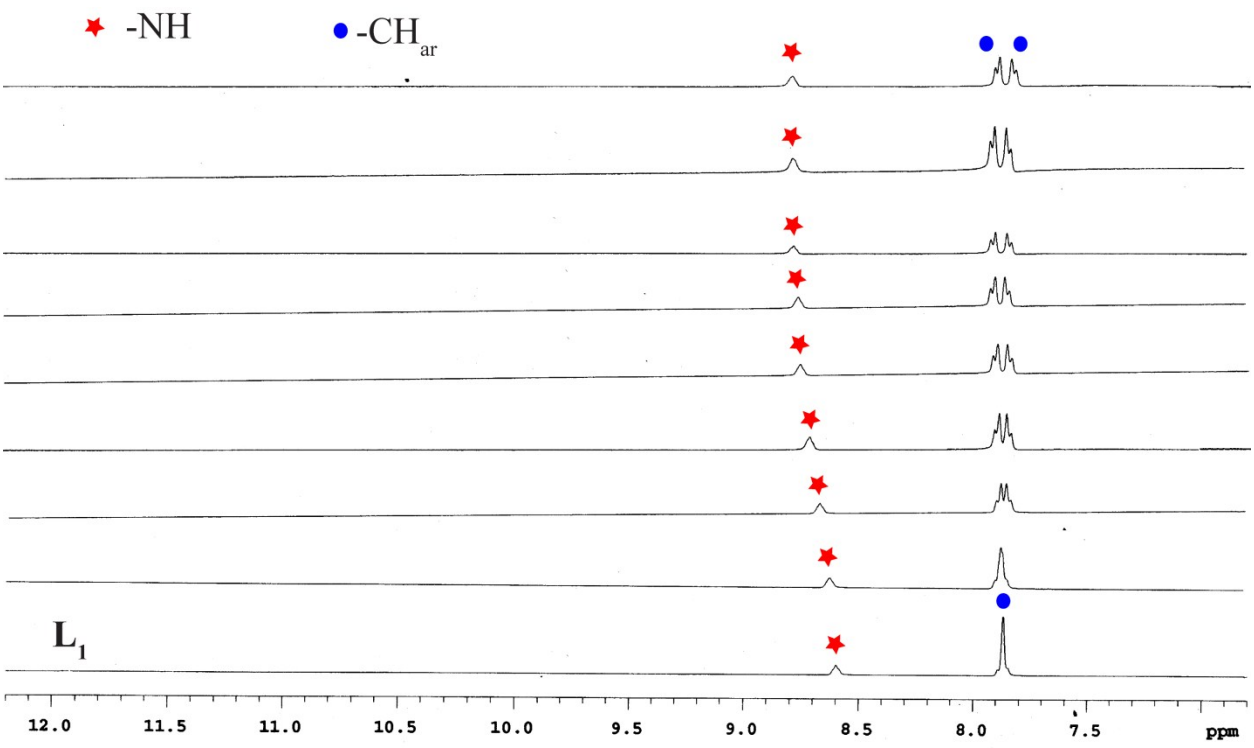

Fig. S40 Stack plot of the ^{1}H NMR spectra of receptor $\mathbf{L_1}$ in the presence of increasing amounts of [*n*-Bu_4N^+]$H_2PO_4^-$ recorded in DMSO-d_6 at 298 K.

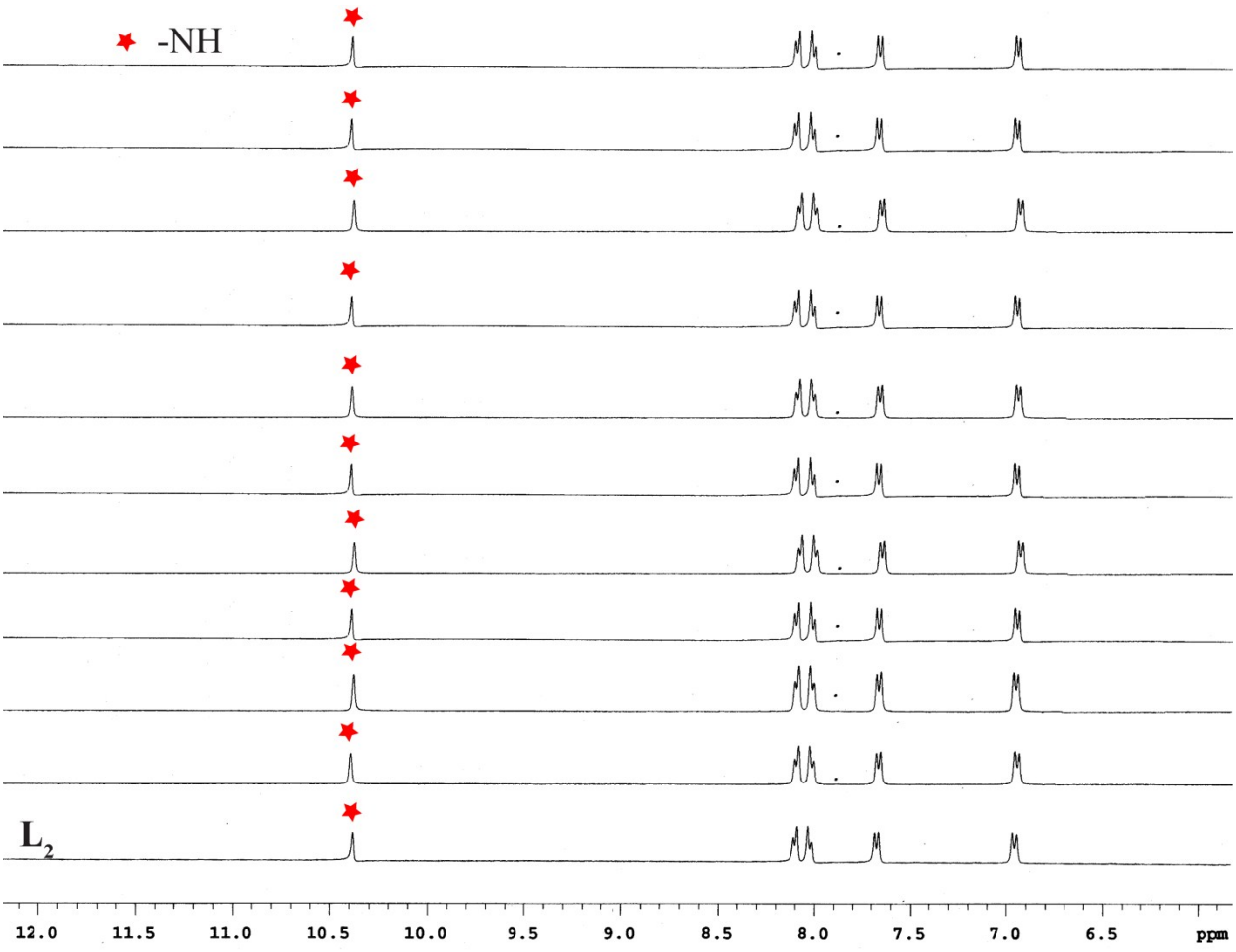

Fig. S41 Stack plot of the ^{1}H NMR spectra of receptor $\mathbf{L_2}$ in the presence of increasing amounts of [*n*-Bu_4N^+]Cl^- recorded in DMSO-d_6 at 298 K.

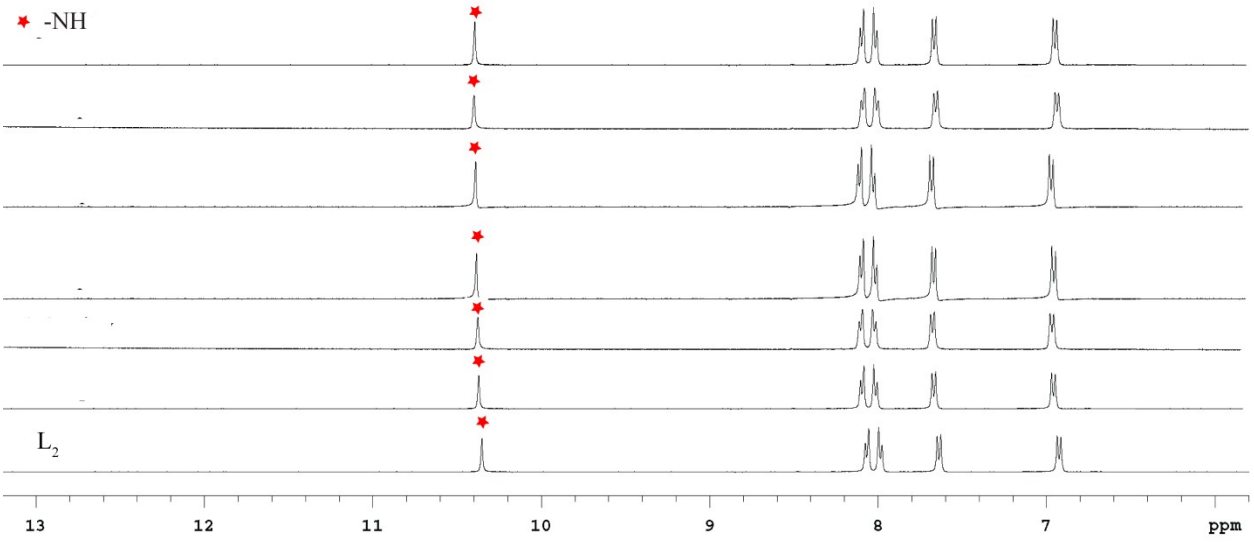

Fig. S42 Stack plot of the ^{1}H NMR spectra of receptor $\mathbf{L_2}$ in the presence of increasing amounts of [*n*-Bu_4N^+]NO_3^- recorded in DMSO-d_6 at 298 K.

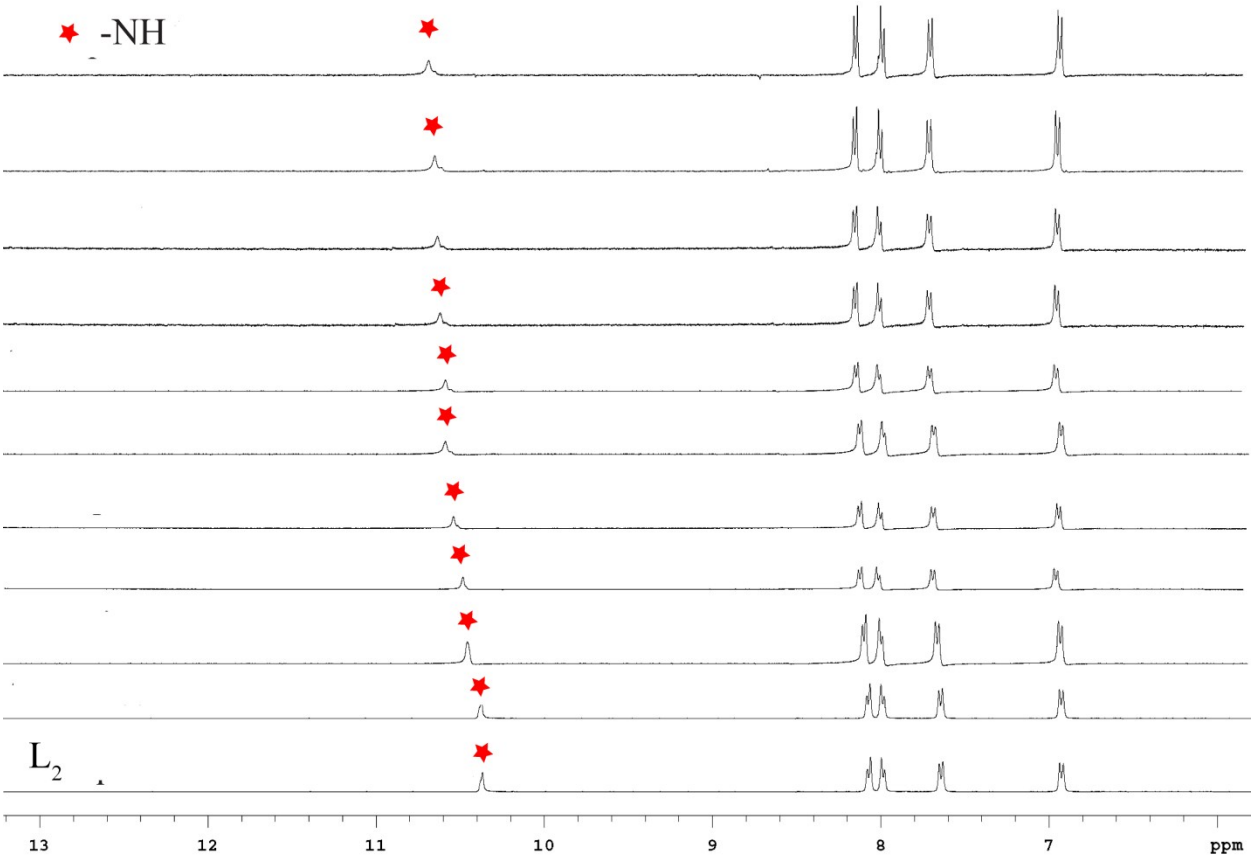

Fig. S43 Stack plot of the ^{1}H NMR spectra of receptor $\mathbf{L_2}$ in the presence of increasing amounts of [*n*-Bu_4N^+]$H_2PO_4^-$ recorded in DMSO-d_6 at 298 K.

Table S1 Crystallographic Parameters for the Crystal Structures **1-5**.

code name	**L_1(1)**	**[L_1H·Br] (2)**	**[L_1H·I] (3)**	**[(L_1H)$_2$·2NO_3·H_2O](4)**	**[L_1H·ClO_4] (5)**
empirical formula	$C_{30}H_{27}N_7O_3$	$C_{30}H_{28}N_7O_3Br$	$C_{30}H_{28}N_7O_3I$	$C_{60}H_{58}N_{16}O_{13}$	$C_{30}H_{28}$ N_7O_7Cl
formula weight	533.59	614.49	661.49	1211.21	634.04
cryst syst	monoclinic	triclinic	triclinic	triclinic	triclinic
a (Å)	19.7331(5)	7.6711(5)	7.7036(7)	7.7878(5)	7.7883(13)
b (Å)	14.8638(5)	11.9923(9)	12.0659(11)	11.9857(8)	12.119(2)
c (Å)	19.2351(6)	16.3251(11)	16.4604(14)	16.6759(12)	16.814(3)
α (degree)	90.00	71.874(5)	72.706(5)	71.155(4)	73.176(10)
β (degree)	100.017(2)	85.255(5)	84.786(5)	84.920(4)	84.484(9)
γ (degree)	90.00	87.127(5)	86.852(5)	88.018(4)	86.573(11)
V (Å^3)	5555.8(3)	1421.92(17)	1454.2(2)	1467.31(17)	1511.2(5)
space group	*C 2/c*	*P -1*	*P -1*	*P -1*	P -1
Z value	8	2	2	2	2
ρ(cal)(g/cm^3)	1.276	1.435	1.511	1.368	1.393
μ(Mo Kα) (mm^{-1})	0.086	1.490	1.145	0.101	0.186
T(K)	298(2)	298(2)	298(2)	298(2)	298(2)
R1; wR2 (I> 2 σ(I))	0.0531, 0.1301	0.0421, 0.0766	0.0583, 0.1199	0.0650, 0.2003	
R1; wR2(all)	0.1086, 0.1557	0.0821, 0.0875	0.1314, 0.1429	0.1004, 0.2364	0.0832, 0.2649
Residual electron density(e/Å)	0.164/-0.245	0.312/-0.395	1.149/-1.186	0.498/ -0.477	0.1324, 0.3068
good-of-fit	1.015	0.990	0.908	0.946	1.096
reflection collected	3510	3629	3466	3199	4410
Independent reflection	6812	5801	6798	5612	7453
CCDC No.	1041356	1041357	1041358	1041359	1041360

Table S2 Crystallographic Parameters for the Crystal Structures **6-10**.

code name	**4LH·4HF$_2$·3 H$_2$O(6)**	**L$_2$H·Br (7)**	**L$_2$H·NO$_3$·H$_2$O (8)**	**L$_2$H·ClO$_4$ (9)**	**(L$_2$H)$_2$·SiF$_6$·4H$_2$ 0·2DMF (10)**
empirical formula	$C_{192}H_{172}F_8N_{28}O_{27}$	$C_{48}H_{40}N_7O_6Br$	$C_{48}H_{42}N_8O_{10}$	$C_{48}H_{40}N_7O_{10}Cl$	$C_{102}H_{94}F_6N_{16}O_{18}Si$
formula weight	3455.58	890.77	890.88	910.32	1982.09
cryst syst	monoclinic	triclinic	monoclinic	monoclinic	triclinic
a (Å)	28.7467(16)	9.4588(5)	16.7671(5)	15.9320(10)	13.0320(8)
b (Å)	18.6826(16)	13.6915(7)	18.6175(5)	18.5172(6)	13.7659(9)
c (Å)	16.7739(11)	20.4866(10)	28.0023(10)	36.597(2)	15.5660(11)
α (°)	90.00	91.493(3)	90.00	90.00	99.496(5)
β (°)	111.627(4)	94.733(2)	102.197(3)	98.905(6)	108.367(5)
γ (°)	90.00	103.295(2)	90.00	90.00	101.296(5)
V (Å^3)	8374.5(10)	2570.4(2)	8543.9(5)	10666.6(10)	2520.6(3)
space group	*C 2/c*	*P -1*	*I 2/c*	*P 21/a*	*P -1*
Z value	2	2	8	8	1
ρ(cal)(g/cm^3)	1.370	1.151	1.382	1.134	1.306
μ(Mo Kα) (mm^{-1})	0.099	0.849	0.099	0.129	0.109
T(K)	298(2)	298(2)	298(2)	298(2)	298(2)
R1; wR2 (I> 2 σ(I))	0.0519, 0.1892	0.0573, 0.1704	0.0711, 0.2733	0.0977, 0.2061	
R1; wR2(all)	0.0859	0.0874, 0.1852	0.1103, 0.3150	0.2438, 0.2866	0.0732, 0.1985
Residual electron density(e/Å)	0.31/ -0.27	1.435/-0.322	0.414/-0.381	0.436/-0.220	0.1958, 0.2639
good-of-fit	1.158	1.031	1.094	0.987	1.040
reflection collected	4867	7346	5935	15793	6677
Independent reflection	8756	13138	10907	27403	10949
CCDC No.	1041361	1041362	1041363	1041364	1041365